J Neurophysiol 110: 952–963, 2013.
First published May 22, 2013; doi:10.1152/jn.00764.2012.

Differences in spectral profiles between rostral and caudal premotor cortex when hand-eye actions are decoupled

Patricia F. Sayegh,[1,2] Kara M. Hawkins,[1,2] Kari L. Hoffman,[2,3] and Lauren E. Sergio[1,2]
[1]*School of Kinesiology and Health Science, York University, Toronto, Ontario, Canada;* [2]*Centre for Vision Research, York University, Toronto, Ontario, Canada; and* [3]*Department of Psychology, York University, Toronto, Ontario, Canada*

Submitted 30 August 2012; accepted in final form 20 May 2013

Sayegh PF, Hawkins KM, Hoffman KL, Sergio LE. Differences in spectral profiles between rostral and caudal premotor cortex when hand-eye actions are decoupled. *J Neurophysiol* 110: 952–963, 2013. First published May 22, 2013; doi:10.1152/jn.00764.2012.—The aim of this research was to understand how the brain controls voluntary movement when not directly interacting with the object of interest. In the present study, we examined the role of premotor cortex in this behavior. The goal of this study was to characterize the oscillatory activity within the caudal and rostral subdivisions of dorsal premotor cortex (PMdc and PMdr) with a change from the most basic reaching movement to one that involves a simple dissociation between the actions of the eyes and hand. We were specifically interested in how PMdr and PMdc respond when the eyes and hand are decoupled by moving along different spatial planes. We recorded single-unit activity and local field potentials within PMdr and PMdc from two rhesus macaques during performance of two types of visually guided reaches. During the standard condition, a visually guided reach was performed whereby the visual stimulus guiding the movement was the target of the reach itself. During the nonstandard condition, the visual stimulus provided information about the direction of the required movement but was not the target of the motor output. We observed distinct task-related and topographical differences between PMdr and PMdc. Our results support functional differences between PMdr and PMdc during visually guided reaching. PMdr activity appears more involved in integrating the rule-based aspects of a visually guided reach, whereas PMdc is more involved in the online updating of the decoupled reach. More broadly, our results highlight the necessity of accounting for the nonstandard nature of a motor task when interpreting movement control research data.

cognitive motor integration; local field potentials; neurophysiology; nonstandard reaching; premotor cortex

REACHING MOVEMENTS RELY on a network of brain regions including the dorsal premotor cortex (PMd) and superior parietal lobule (SPL) (Battaglia-Mayer et al. 2001; Caminiti et al. 1999; Kalaska et al. 1998). It is not well understood how activity within this network is modulated during a reaching movement when there is a dissociation between the actions of the eyes and hand, termed a "nonstandard" movement (Wise et al. 1996). There is strong evidence that the actions of the eyes and hand are tightly linked (Gauthier and Mussa Ivaldi 1988; Gielen et al. 1984; Gorbet and Sergio 2009; Henriques et al. 1998; Morasso 1981; Neggers and Bekkering 2000; Prablanc et al. 1979; Sergio and Scott 1998; Terao et al. 2002; Vercher et al. 1994); hence, the brain must employ specific mechanisms to break this link during nonstandard movements (Murray et al. 2000; Sergio et al. 2009; Wise et al. 1996). Inhibition of this linkage likely depends on neural circuitry that is different from but interconnected with the circuitry important for controlling natural reaching movements (Clavagnier et al. 2007; Gail et al. 2009; Sergio et al. 2009). Support for this idea comes from the observation that decoupled eye-hand coordination develops only later in childhood (Bo et al. 2006; Piaget 1965; Sergio et al. 2009), that movement slows and accuracy declines when eye and hand movements are decoupled (Epelboim et al. 1997; Goodbody and Wolpert 1999; Gordon et al. 1994; Henriques et al. 1998; Messier and Kalaska 1997; Terao et al. 2002), and that patients with neurological disorders show impaired nonstandard reaching while standard reaching is largely unaffected (Ghilardi et al. 1999; Halsband and Passingham 1982, 1985; Jackson et al. 2005; Karnath and Perenin 2005; Tippett and Sergio 2006; Tippett et al. 2007).

Cell activity in PMd is modulated by gaze direction, wrist orientation, hand direction, and intended movement kinematics (Boussaoud 2001; Boussaoud and Wise 1993a, 1993b; Boussaoud et al. 1998; Caminiti et al. 1990; Cisek and Kalaska 2002; Raos et al. 2004). Recent findings suggest that the rostral and caudal subdivisions of PMd (PMdr and PMdc) have separate roles in the visuomotor transformation needed to plan an upcoming visually guided reach (Raos et al. 2004). These results are strengthened by anatomic studies demonstrating that PMdr and PMdc have separate cortical connections. PMdr has strong reciprocal connections with prefrontal regions (Lu et al. 1994), whereas PMdc has strong connections to the primary motor cortex and the spinal cord (Barbas and Pandya 1987; Geyer et al. 2000; Luppino et al. 1990); therefore, PMdc may be involved in coding limb movement parameters (Alexander and Crutcher 1990; Cisek et al. 2003). In contrast, PMdr may have a role in the context-dependent selection and planning of movements in conditions that involve nonstandard mappings (Boussaoud 2001; Cisek and Kalaska 2005; Raos et al. 2004), although this remains to be tested directly.

Oscillatory activity within the local field potential (LFP) has been used to measure many neuronal processes such as attention, memory, action, and perception (Baker et al. 1999; Brovelli et al. 2005; Cooper et al. 2003; Donoghue et al. 1998; Jensen et al. 2007; O'Leary and Hatsopoulos 2006). LFPs represent the activity within local cell assemblies (Scherberger et al. 2005) and are believed to represent the input into an area (Scherberger et al. 2005). Since spiking activity reflects suprathreshold inputs or outputs from pyramidal cells, it is very likely that spike and LFP recordings carry different sets of information and can therefore be complementary tools for brain analysis (Pesaran et al. 2002; Sanes and Donoghue 1993). In fact, some researchers have concluded that LFP activity is

Address for reprint requests and other correspondence: L. E. Sergio, 4700 Keele St., 357 Bethune College, Toronto, ON, Canada M3J 1P3 (e-mail: lsergio@yorku.ca).

more accurate than spike activity when decoding certain behavioral states (Mitzdorf 1985). Another benefit to LFP analysis is its strong relationship with blood oxygen level-dependent (BOLD) functional magnetic resonance imaging (fMRI) activity in humans (Goense and Logothetis 2008; Nir et al. 2007) and with spike activity in nonhuman primates (Fries et al. 2001). The relationship between LFP, spike, and BOLD activity can be used to bridge the gap between neurophysiological data in animals (single-cell recording) and human fMRI recordings.

In the present study, we examine how oscillatory and spike activity within PMd are modulated when gaze and hand motions are spatially incongruent, relative to more natural spatially congruent reaches. In addition to overall changes in the spectral profile as a consequence of nonstandard reaching, we predict that the rostral subdivision of PMd will show greater modulation relative to the caudal subdivision, particularly during the planning phases of the nonstandard task.

METHODS

Apparatus and Behavioral Task

Two rhesus monkeys (female *Macaca mulatta*, *monkeys A* and *B*, body weight 5.2 kg) were trained to perform visually instructed, delayed reaching tasks in standard and nonstandard conditions. All surgical and animal handling procedures were in accordance with Canadian Council on Animal Care guidelines on the use of laboratory animals and were preapproved by the York University Animal Care Committee.

During the experiment, the monkey was seated in a custom-built primate chair 40 cm in front of a 38.1-cm vertical screen, which was set at monkey eye level and centered with her midline. An additional 38.1-cm horizontal touch-sensitive screen (Touch Controls, San Diego, CA) was set in front of the animal, between the animal's waist and xyphoid process, so that she could reach over the entire surface of the screen comfortably (Fig. 1). The horizontal touch screen was designed to detect spatial displacements as small as 3 mm using infrared beams at a sampling rate of 100 Hz. Continuous tracking of the eye was performed using the ISCAN-ETL 200 Eye Tracking System (ISCAN, Burlington, MA) at a sampling rate of 60 Hz. Performance in both conditions required the animals to reach toward one of eight peripherally cued targets on the horizontal touch screen. The animals were trained to perform similar movements during both conditions, and the biomechanical features of the reach movements were monitored to ensure that the movement profiles were similar between conditions. In addition, to minimize any interference from the nonreaching limb, the animals were trained to maintain their nonreaching hand on a metal lever just beyond the lower corner of the horizontal touch screen. In this way it was ensured that the animals only used the appropriate arm without the unused limb having to be forcefully restrained.

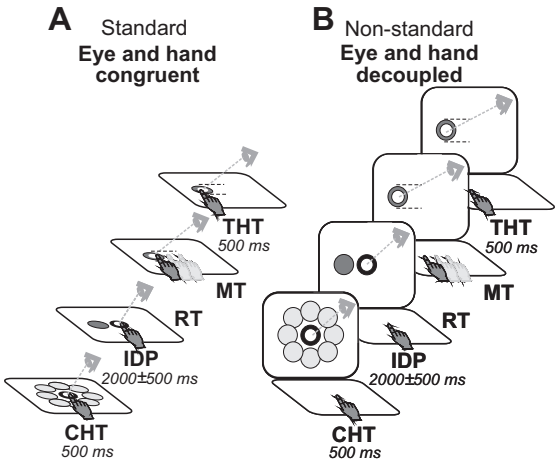

Fig. 1. Experimental setup and trial timing. *A*: schematic of standard condition. *B*: schematic of nonstandard condition. During each trial, 1 of 8 equally spaced (45°) peripheral targets was presented on either a touch-sensitive screen placed over the animal's lap (*A*) or on a monitor positioned vertically 40 cm away from the animal's frontal plane (*B*). Arm movements were always made over the horizontal touch screen. Light gray circles represent the 8 possible target locations (not illuminated before cue). Epochs: CHT, center hold time; IDP, instructed delay period; RT, reaction time; MT, movement time; THT, target hold time. The animal's head was fixed throughout the experiment.

The visual targets were identical across conditions, but the spatial plane of presentation was altered. At the start of each trial, a red circular target (70 mm in diameter) appeared at the center of the screen with an additional smaller white circular target (40 mm in diameter; 5.7° of visual angle) on top of it. The red target instructed where the monkey should touch, and the white target instructed where the animal should maintain eye fixation. After a baseline period of 500 ms, one of eight green-colored peripheral targets appeared (70 mm in diameter). All eight targets were equally spaced (45°) and appeared randomly, based on a randomized-block design. The peripheral target appeared 5 times at each location for a total of 40 trials per condition. After a variable instructed delay period (IDP; 2,000 ± 500 ms), the red central target extinguished and the white target jumped to the peripheral target. This served as the go signal (GO) instructing the animal to move the eyes and hand from the central target to the peripheral target (Fig. 1). The movements were made from the center of the central target to the center of the peripheral target (roughly 80 mm; see Fig. 2). Once the eyes and hand arrived at the peripheral target, the monkey was required to hold them there for 500 ms, after which a liquid reward was delivered to the animal. In addition, to reinforce similar hand paths between conditions, movement alleys were included to ensure that reaches were directed along a fairly straight trajectory. These alleys were set at ±40 mm from a straight line spanning from the central to the peripheral targets. If the monkey's hand deviated beyond the set alley, the trial was stopped. To provide feedback on the current position of the hand, a crosshair representing the position of the finger on the touch screen was displayed.

In the standard condition, the actions of the eyes and hand remained congruent. The visual presentation of the task and the reaching movements were both made on the horizontal touch-sensitive screen placed in front of the animal (Fig. 1*A*). In the nonstandard condition, the actions of the eyes and hand were decoupled: the visual presentation of the task was on the vertical screen while the animal's limb movement remained on the horizontal touch screen (Fig. 1*B*). Thus the animal was required to direct its gaze along the vertical monitor but move its finger along the horizontal monitor to displace the cursor from the central to the peripheral target. To ensure that the animal did not track its hand position extrafoveally, an opaque screen was placed 10 cm above the animal's arm to block vision of the limb. For each condition, two epochs during the trial were considered, the instructed delay epoch (IDP) and the movement epoch (MOVE). IDP comprised the 500 -ms baseline period and the first 1,000 ms of the instructed delay. MOVE comprised the last 500 ms of the instruction delay up until 500 ms after movement onset.

We also had a gaze-only condition, to determine if the oscillatory activity within the subregions of PMd was affected solely by the overall shift in gaze angle between conditions. Gaze-only data were collected for every recording. The visual display consisted of nine white circles (40 mm in diameter, 5.7° of visual angle) that appeared in the same locations as the white targets that appeared during the experimental conditions. The monkey was instructed to fixate on each of these white circles while maintaining both hands beside the hori-

zontal touch screen. The white circles appeared one at a time in each location 3 times for a total of 27 saccades for each plane.

Muscle activity was recorded from 13 proximal arm muscles in separate recording sessions. Pairs of Teflon-insulated 50-μm single-stranded stainless steel wires were implanted percutaneously. Implantations were verified by passing current through the wires to evoke focal muscular contractions ($<$1.0-mA, 30-Hz, 300-ms train; Sergio and Kalaska 2003). Multi-unit electromyography (EMG) activity was amplified, band-pass filtered (100–3,000 Hz), half-wave rectified, integrated (5-ms time bins), and digitized online at 200 Hz. The muscles studied included the anterior deltoid, medial deltoid, posterior deltoid, dorsoepitrochlearis, infraspinatus, latissimus dorsi, pectoralis, supraspinatus, teres major, rostral trapezius, caudal trapezius, triceps lateralis, and triceps medialis. These recordings were performed to assess the general effects of the standard and nonstandard tasks on EMG activity and were not designed as a definitive biomechanical study of the muscle properties.

Behavioral and Muscle Data Analysis

Hand paths recorded from the touch-sensitive monitor were analyzed to confirm that the movements were biomechanically similar between conditions. The individual movement paths were first low-pass filtered at 10 Hz, and the movement onsets and endpoints were automatically scored as 8% peak velocity at the beginning and end of the velocity profile, respectively. The movements were then cut at the onsets and endpoints and divided into 21 equal segments. The five trials for each direction were then pooled, and the means and standard deviations were calculated at each segment along the path. An equality of variance test was performed between the two conditions on the mean x and y components of the trajectory for each target (Snedecor and Cochrane 1989). Since a given trial was only kept if the animal went from the central to the peripheral target within a somewhat narrow alleyway, this test determined if, despite this behavioral training, there were any systematic differences in movement variability between tasks. Mean reaction times (from the GO signal to 8% peak velocity) were also calculated for each condition, and paired-samples t-tests were performed to compare reaction times between the standard and nonstandard conditions. Repeated-measures ANOVAs were performed on the EMG data during the IDP and MOVE epochs for each muscle recorded to determine the effect of target (motion direction) and condition (standard and nonstandard) on maximum EMG amplitude. It was expected that reach direction would have an effect on EMG amplitude but that condition would not.

Neural Recordings

Monkeys were implanted with a recording cylinder under standard aseptic surgical techniques (Kalaska et al. 1989). Briefly, a Plexiglas cylinder (used to hold the electrode manipulandum) was positioned on the 19-mm craniotomy and fixed into place using cranioplastic acrylic and titanium neurosurgical screws. A small metal fixation pole used to stabilize the head during recording was also implanted into the acrylic. The stereotaxic coordinates for chamber placement over PMd (both monkeys: interaural anteroposterior, +16 mm; mediolateral, +11 mm) were determined using *The Rhesus Monkey Brain in Stereotaxic Coordinates* (Paxinos et al. 2000). The border between rostral and caudal PMd and primary motor cortex (M1) was drawn according to previously proposed physiological and cytoarchitectonic criteria (Fujii et al. 2000). The experiments began a week after surgery following a complete recovery.

LFPs and single units were collected from the extracellular recordings within PMd. A hydraulic multichannel driver (MCM-4; FHC, Bowdoin ME) mounted to the implanted chamber was used in conjunction with a multichannel processing system (MCP; Alpha-Omega Engineering, Nazareth, Israel). Standard tungsten microelectrodes (impedance 1–3 MΩ; FHC) were used for recording the neural activity within PMd. The multidriver provided simultaneous recordings from up to two penetration sites at a time. Neural activity from each electrode was preamplified (5,000 times), band-pass filtered (1 Hz–10 kHz), and split into lower (LFP) and higher (single units) frequencies. Higher frequency signals were sampled at 12.5 kHz and passed through the multispike detector (Hawkins et al. 2013). The lower frequency signals (below 100 Hz) were sampled at 390.6 Hz.

Data Analyses

Directional tuning was determined on the basis of previously described methods (Georgopoulos et al. 1982; Hawkins et al. 2013). Briefly, a sinusoidal regression on the mean discharge rates for each target direction was performed, and the goodness of the regression fit was calculated. The regression equation was then reexpressed in terms of the peak of the sine wave, which is the direction for which the cell was most active (i.e., the "preferred direction") (Georgopoulos et al. 1982). A bootstrap test was then performed using 1,000 shuffled activities to determine the significance of the tuning based on a 95% confidence interval (CI). The mean firing rates of each cell were then normalized to each cell's individual mean baseline firing rate. The baseline firing rate was calculated as the mean firing rate during the first 300 ms of each trial when the animal was instructed to hold its hand at the central target. This generated a normalized firing rate for comparison with the LFP data, which were also normalized to the same baseline time period (see below). Significance was determined by performing a three-way mixed ANOVA with condition (standard vs. nonstandard) and time (early vs. late) as within-subject factors and location (PMdr vs. PMdc) as between-subject factor. All ANOVA results were reported with Greenhouse-Geisser-corrected P values, and post hoc comparisons were corrected for multiple comparisons (Bonferroni). All successfully recorded LFP sites were included in all analyses. The converted data were analyzed in MATLAB (The MathWorks, Natick, MA) using both custom-written and open-source (Chronux.org) programs. Chronux script files were used to analyze the spectral profiles and generate time-frequency spectrograms for all penetrations for both conditions (Jarvis and Mitra 2001; Pesaran et al. 2002). We used spectral analysis to categorize the power at different frequency bands. To estimate the frequency structure of the LFP activity, we used the multitaper spectrum analysis (previously described by Jarvis and Mitra 2001; Pesaran et al. 2002). The multitaper technique provides an optimal estimate of the spectrum by reducing spectral leakage and variance of the estimate by averaging the spectral estimates from several orthogonal tapers (Jarvis and Mitra 2001). The orthogonal tapers are Slepian np prolate functions (Jarvis and Mitra 2001). A Fourier transform was then applied to the tapered signal. The multitaper estimates of the spectrum Sx(f) for each recording were then calculated (Pesaran et al. 2002; Scherberger et al. 2005). The spectrum was z-transformed to the baseline period, which consisted of 300 ms at the start of each trial during which time the animal was maintaining eyes and hand at the central target. Normalizing to a baseline period was necessary to compare between conditions and locations. No significant differences were observed between baseline activity when comparisons were made between conditions within each region ($P > 0.05$). Spectrograms were calculated using a 200-ms window shifted in 50-ms increments with a 3-Hz frequency resolution. Mean spectra reflect the spectra z-transformed from individual trials and then collapsed across target directions and electrode sites within the respective PMd region.

To determine the statistical significance of task-related differences ($P < 0.05$), the normalized spectrum from each electrode site was divided into four frequency bands (0–10, 10–30, 30–45, and 45–70 Hz). Data from above 70 Hz were not presented because the pattern of activity within this range has been shown to be closely related to spiking activity (Ray and Maunsell 2011; Zanos S et al. 2012; Zanos TP et al. 2011). The average spectral value across time for each frequency band was determined for each condition (standard and

nonstandard). A bootstrapping procedure was used to assess whether the difference in power between the two conditions could have occurred by chance, based on the assumption that if power was the same between the two conditions, then the distribution of differences of the bootstrapped estimates of LFP power between conditions would be normally distributed and centered around zero difference. This test was implemented as follows. The empirical estimate of power was obtained by calculating the power difference between standard and nonstandard conditions. A bootstrapped distribution was created by random reassignment of the condition label (standard/nonstandard) for each observation within these distributions and the mean power difference recalculated. This was repeated 1,000 times to generate a distribution of 1,000 bootstrapped power difference values that could be expected if the observed power differences were due to chance (i.e., random condition assignment). The bootstrapped differences were then rank ordered. The high and low limits of the 95% CI were defined as the 25th and 975th largest power values (2-tailed test). Activity from an electrode site was considered to have undergone a significant shift in power between conditions if the calculated power difference between conditions fell outside of the 95% CI of the distribution of its bootstrapped LFP powers (i.e., the null hypothesis that the mean value for power of 0 can be rejected at alpha = 0.05, 2-tailed test). The time points and frequency ranges that were significantly different between standard and nonstandard conditions were recorded. To generate spectrograms that displayed the task related differences, we subtracted the standard from the nonstandard spectrum for each site and averaged across the population for each region. All values that were not significant were set to zero, any value above zero represents stronger power for that time-frequency bin within the standard condition, and any value below zero represents stronger power within the nonstandard condition, using an alpha value of 0.05.

To determine topographical differences between PMdr and PMdc, we compared the activity between each region during each condition. The same methods were used as the ones described for the task-related analysis; however, bootstrapping was done between PMdr and PMdc for each condition.

Last, we analyzed the oscillatory activity in the gaze-only condition to determine if the overall shift in gaze angle that occurred between the two planes associated with each conditions had an effect on the oscillatory activity within PMd. All recorded sites from PMdr and PMdc were tested in gaze-only conditions. Only a subportion of these sites was used for this analysis. The mean power (0–70 Hz) at each gaze location was calculated from a 500-ms window while the animal was fixating at each target. Within each condition, the mean power across the nine target locations was computed. A bootstrapping procedure was used to assess whether the difference in power between the two gaze planes could have occurred by chance (for details see above).

RESULTS

The current results demonstrate changes in the neural activity within PMd when a coupled vs. decoupled reaching movement is performed. The change in neural activity differed between PMdr and PMdc, suggesting functional differences between these regions. These results did not arise from differences in limb biomechanics or gaze angle and support our hypothesis that these regions are involved in visuomotor transformations for nonstandard mapping.

Behavioral Results

To ensure that any oscillatory differences seen between conditions were not a result of differences in the movement of the hand, we compared hand trajectories between conditions. We wanted to ensure that the biomechanical features of the limb movements were identical throughout the experiment. This guarantees that the interpretations of the LFP data are not affected by a difference in limb movements. The use of alleys helped support the animal in maintaining similar hand trajectories during both conditions (see METHODS). Figure 2*A* shows the mean reach trajectories during both conditions for each animal. Except for a few segments, there were no significant differences in the reach trajectories between standard and nonstandard conditions. An analysis of the EMG data revealed that for 11 of 13 muscles there was no main effect of condition during the IDP and MOVE epochs ($P > 0.01$). For two muscles, medial deltoid and teres major, there was a marginal effect of condition on EMG activity during the IDP epoch ($0.05 > P > 0.01$). This may have been due to a slight alteration in the animals' starting posture in reaction to the board placed over their arm in the nonstandard condition. There was, as expected, a main effect of target for all proximal arm muscles studied during the movement epoch ($P < 0.01$). Finally, reaction times between the standard (537.9 ± 12.82,

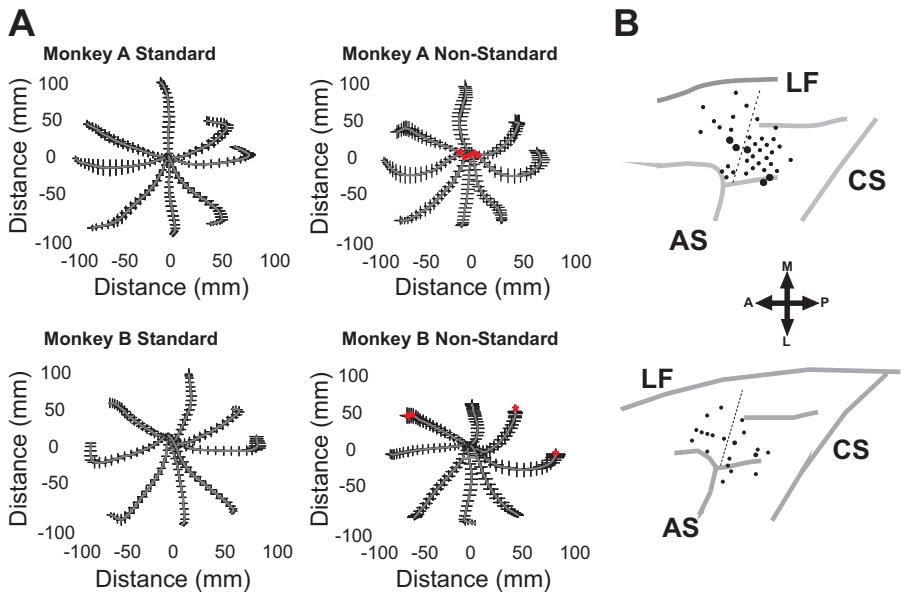

Fig. 2. *A*: mean reach trajectories. Gray lines indicate mean movement trajectories; black tick marks indicate SD. Red asterisks denote trajectory segments that were significantly ($P < 0.05$) more variable compared with the standard condition. *B*: penetration sites for *monkey A* (*top*) and *monkey B* (*bottom*). Larger circles indicate where recordings were obtained on 2 occasions. AS, arcuate sulcus; CS, central sulcus; LF, longitudinal fissure. Arrows show anterior (A), posterior (P), medial (M), and lateral (L) directions; dotted line denotes division between penetration sites classified as rostral (left of line) or caudal (right of line).

mean ± SE) and nonstandard (522 ± 9.89) conditions were also not significantly different [$t(45) = 0.927$, $P = 0.359$]. Taken collectively, these results strengthen the conclusion that any neural differences observed between conditions are not a direct result of changes in the biomechanics of the reaching movement, but rather the control of the movement.

Neural Activity

We obtained 66 (59 from *monkey A*, 7 from *monkey B*) LFP recordings and classified 36 of these recordings as coming from PMdr and 30 recordings as coming from PMdc, based on the stereotaxic coordinates of the recording chamber and the penetration location in the chamber (Fig. 2*B*). All successfully recorded LFP sites were included in the analysis. In addition, 52 single cells were recorded within PMd (28 PMdr and 24 PMdc) during both conditions, of which only 29 were found to be task-related (directionally tuned during either the IDP or MOVE epoch). In support of our hypothesis, we observed that oscillatory and single-unit activity in PMd were modulated by the type of eye-hand coordination: standard (direct object interaction) or nonstandard (decoupled effectors). In addition, we observed that the temporal and spectral profile of change depended on the region (rostral or caudal) of PMd sampled.

Task-Related Differences Within PMd

Oscillatory activity. Our first main finding was that we observed salient differences in the oscillatory activity during performance under the standard condition compared with the nonstandard condition in both subregions of PMd. We analyzed the neural activity within two epochs (see METHODS). During the IDP epoch, the animal received information about the location of the peripheral target but was required to maintain hand and eye position at the central location. Thus during this epoch the early stages of movement planning would be occurring. Figure 3 shows an example of the increase in power that occurs across each frequency band for a single PMdc recording site during both epochs. An example spectrum from each animal for each epoch is also shown in Fig. 3, *C* and *D*, to demonstrate the similarity in spectral profile between animals. Because of these similarities, all analyses were pooled between animals. The MOVE epoch represents both the very late stages of planning and the early stages of the movement (see METHODS). During this epoch the movement has already been planned and there is an anticipation of the GO signal. Additionally, the second 500 ms of this epoch represents the first 500 ms of the reaching movement, which was the same

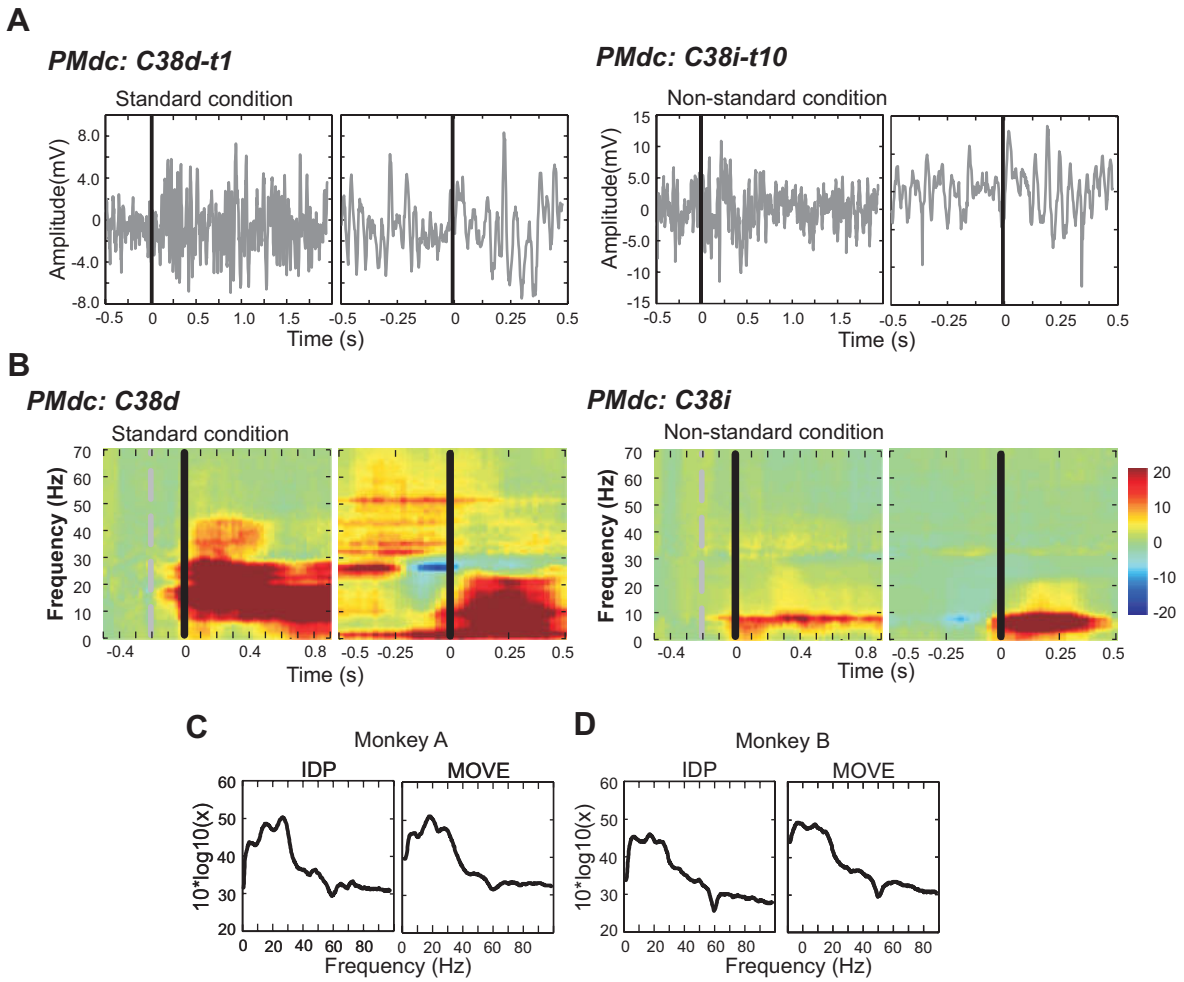

Fig. 3. Example recordings for a site on the caudal portion of dorsal premotor cortex (PMdc). *A*: example broadband local field potential (LFP) during IDP and movement (MOVE) epochs for both conditions. Black line indicates peripheral target (IDP epoch; *left*) or movement onset (MOVE epoch; *right*). *B*: example time-frequency spectrograms of oscillatory activity during each epoch and condition. *C* and *D*: example spectral power during the IDP and MOVE epochs demonstrating similarity between animals.

between conditions (i.e., only the eye movement coupling varied between conditions; Fig. 1).

During the IDP epoch, changes to the overall oscillatory activity occurred when the eyes and hand were decoupled vs. when they were congruent (Fig. 4, *A–F*, *left*). Shortly after peripheral cue onset (black vertical line), there was an increase in oscillatory activity that occurred in both regions of PMd during both conditions (Fig. 4, *A–D*, *left*). To show task-related differences more clearly, Fig 4, *E* and *F*, display the main differences in power across conditions, masked for significance (see METHODS). We observed a significant increase in PMdr oscillatory power within the 10- to 70-Hz range during the nonstandard condition relative to the standard condition (Fig. 4*E*, *left*; $P < 0.05$). Contrary to this finding, PMdc showed a reduction in oscillatory activity between conditions within the 0- to 45-Hz range (Fig. 4*F*, *left*; $P < 0.05$). Figure 5 displays the *z* score for each frequency bin across time and allows for a more in-depth look at the pattern of change between conditions. As shown in Fig. 4*B*, the oscillatory activity within PMdr shows a greater increase in power during the nonstandard compared with the standard condition (Fig. 5, *B–D*, *top left*; $P < 0.05$). On the other hand, stronger oscillatory activity occurred for the standard compared with the nonstandard condition within PMdc (Fig. 5, *A–C*, *bottom left*; $P < 0.05$).

Our findings during the MOVE period showed more subtle differences in oscillatory activity when the eyes and hand were decoupled (Fig. 4, *A–D*, *right*). Task-related differences were only observed within the 0- to 10-Hz range before movement onset for both PMdr and PMdc (Fig. 4, *E* and *F*, *right*). Both regions showed a significant reduction in oscillatory activity during the nonstandard compared with the standard condition within this frequency range (Fig. 5*A*, *right*; $P < 0.05$). After movement onset, PMdc shows both a reduction of power within the 10- to 30-Hz range (Fig. 5*B*, *bottom right*; $P < 0.05$) and an enhancement of power within the 45- to 70-Hz range (Fig. 5*D*, *bottom right*; $P < 0.05$). These results demonstrate that just before movement, both PMdr and PMdc activity were modulated by decoupling the action of the eyes from the hand. By movement onset these conditional differences were less evident, with PMdc showing slight differences between reaching movements (Fig. 4, *E* and *F*).

Spiking activity. The task-related differences observed within the LFP data are also supported by single-cell findings (Fig. 6). In line with the observed increase in oscillatory activity, a significant increase in firing rate can also be observed within PMdr during the planning phase of a nonstandard compared with a standard reach (Figs. 6*B* and 7*A*; $P < 0.01$). Contrary to the observations in the oscillatory activity within PMdc, a significant increase in firing rate also occurred during decoupled reaching movements within this region (Fig. 7*A*; $P < 0.01$). During the MOVE period, we decided to separate the analysis into an early (before movement) and late period (after movement began) to address whether the spike activity follows the same pattern observed for the LFPs during this MOVE period. In this analysis, we observed that task-related differences in spiking activity occurred only after movement onset in both regions (Fig. 7*B*; $P < 0.01$). PMdc was most active during standard reaching movements, and firing rates decreased during eye-hand decoupling (Fig. 7*B*, late epoch; $P < 0.01$). PMdr, however, showed enhanced spiking activity only following movement onset (late epoch) during nonstandard reaches, whereas standard reaches showed a significant

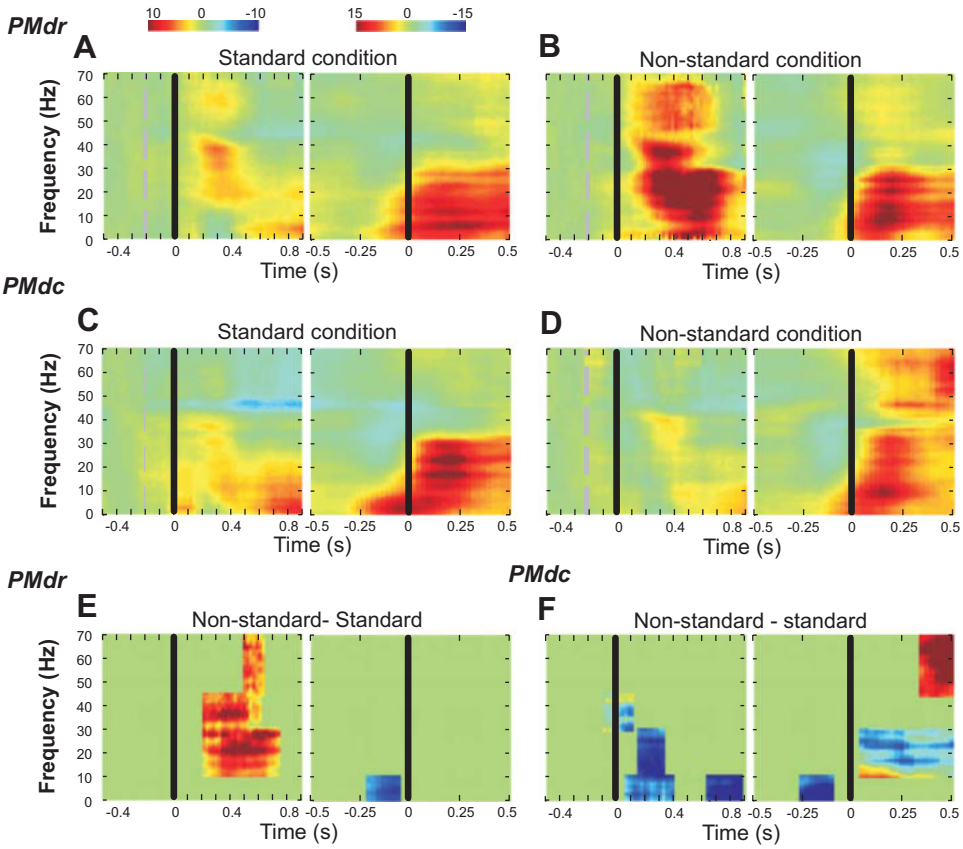

Fig. 4. Population time-frequency spectrograms of oscillatory activity during the IDP and MOVE epochs. *A* and *B*: population spectrograms of power in rostral portion of dorsal premotor cortex (PMdr) during standard (*A*) and nonstandard conditions (*B*). *C* and *D*: population spectrograms of PMdc power for standard (*C*) and nonstandard conditions (*D*). *E* and *F*: population spectrogram showing only significant differences between standard and nonstandard conditions within PMdr (*E*) and PMdc (*F*). Each time-frequency bin was masked at a 95% confidence interval (CI) based on bootstrapped data (see METHODS). Power is color-coded on a log scale. For *E* and *F*, colors coded above 0 indicate greater power within the nonstandard condition, and colors coded below 0 indicate greater power within the standard condition. Black line indicates peripheral target onset during IDP epochs and movement onset during MOVE epochs; gray dashed line indicates end of the baseline period.

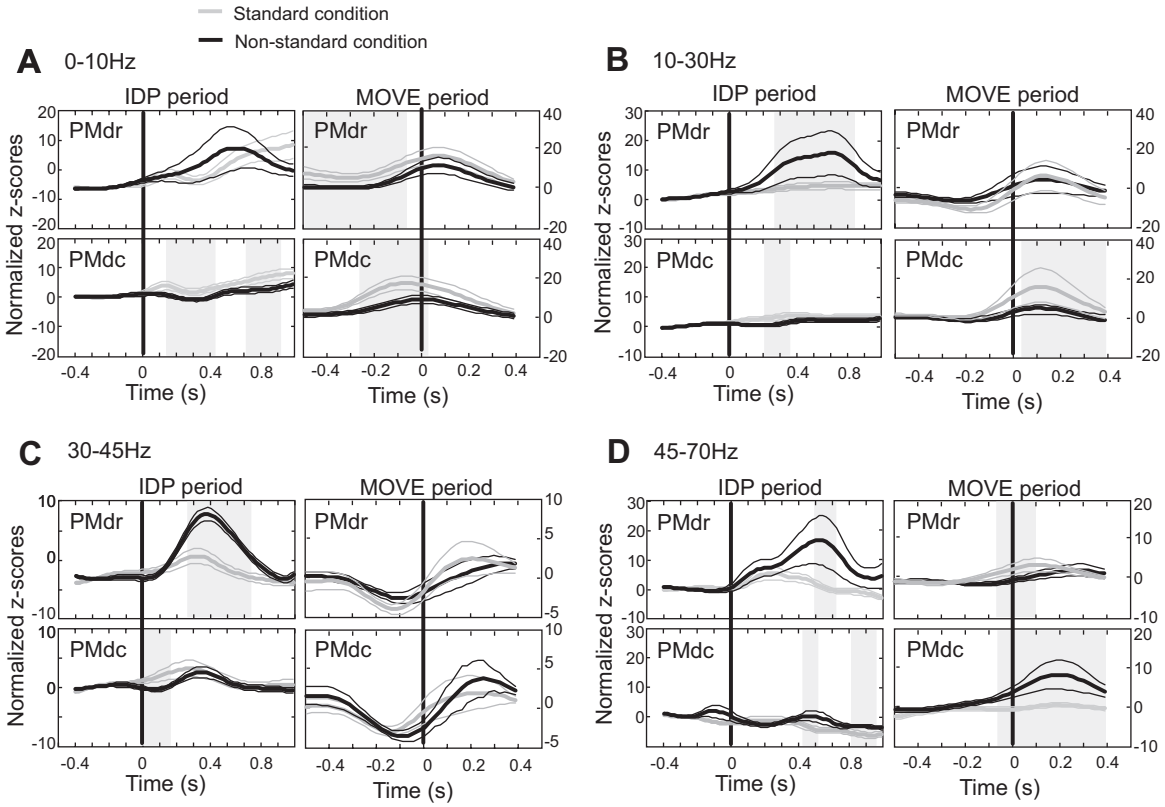

Fig. 5. Time course of task-related differences in power during the IDP (*A–D*, *left*) and MOVE epochs (*A–D*, *right*), segregated by frequency band. *Z*-score values are broken up into frequency ranges of 0–10 (*A*), 10–30 (*B*), 30–45 (*C*), and 45–70 Hz (*D*). Black line represents peripheral cue onset (IDP period) and movement onset (MOVE period). Gray bars indicate when the power was significantly different between conditions ($P < 0.05$).

reduction in mean firing rate (Fig. 7*B*; $P < 0.01$). This suggests that by the late planning stage (early MOVE epoch), task-related differences that occur during the early planning period become absent and movement-related differences are only observed following movement onset.

Topographical Differences in Eye-Hand Decoupling

Oscillatory activity. In support of our hypothesis, we also observed topographical differences between PMdr and PMdc in the modulation of oscillatory activity between conditions. The most striking finding was the significantly greater power in oscillatory activity during eye-hand decoupling within PMdr following peripheral cue onset (Fig. 4*E*, *right*). PMdc, on the other hand, demonstrated a reduction in power when the eyes were decoupled from the hand (Fig. 4*F*, *right*). To more explicitly evaluate these topographical differences during the IDP and MOVE epochs of a given condition, we plotted the relative power differences between regions for each of four frequency bands (Fig. 8). Within the IDP epoch, a similar pattern of oscillatory activity can be seen between regions in the standard condition (Fig. 8*A*). Topographical differences were only observed in the 45- to 70-Hz range (Fig. 8*A*, *left*; $P < 0.05$). During the nonstandard condition, however, clear differences in power can be observed across many frequencies ranges (10–70 Hz; Fig. 8*A*, *right*; $P < 0.05$).

By the late planning and movement stage, PMdr and PMdc once again demonstrate similarity in the pattern of oscillatory activity during both conditions (Figs. 5, *right*, and 8*B*). In

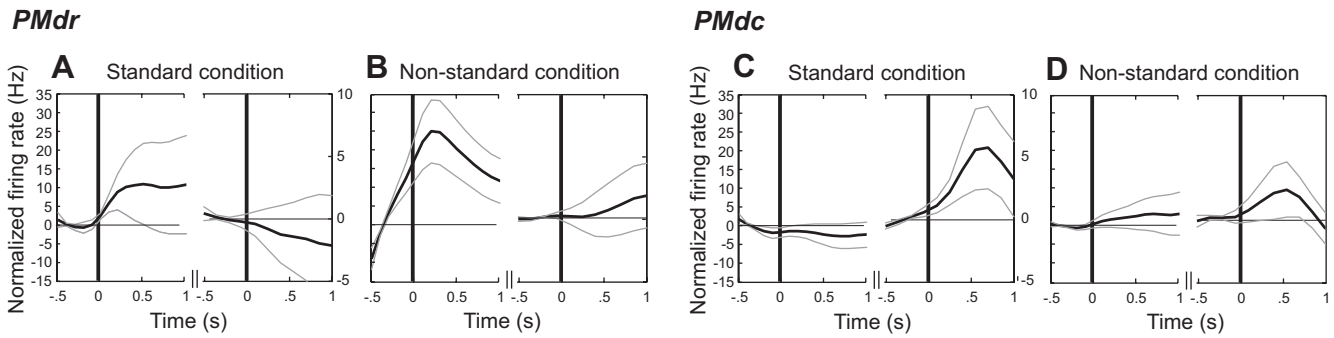

Fig. 6. Mean discharge rates of single cells within PMd across the tasks. *A* and *B*: mean normalized firing rates for PMdr during standard (*A*) and nonstandard conditions (*B*). *C* and *D*: mean normalized firing rates for PMdc during standard (*C*) and nonstandard conditions (*D*). Black lines represent peripheral cue onset during the IDP epoch (*A–D*, *left*) and movement onset during the MOVE epoch (*A–D*, *right*).

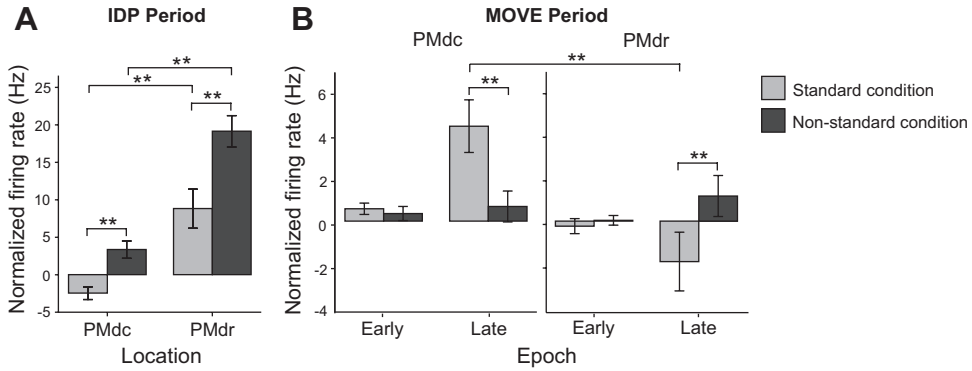

Fig. 7. Histogram demonstrating significant difference in the normalized mean firing rates between conditions and locations. *A*: normalized firing rates as a function of condition and location during the IDP epoch. *B*: normalized firing rates during MOVE epoch broken up into early (before movement onset) and late periods (after movement onset). *$P < 0.05$; **$P < 0.01$, significant difference between either conditions or locations, as indicated.

summary, during the early planning of a nonstandard reach, PMdr shows enhanced oscillatory activity compared with PMdc. By the late planning and early movement phase, although the oscillatory activity within PMdr and PMdc are both modulated between conditions, there were less obvious topographical differences in the way that this activity was modulated.

Spiking activity. In support of our LFP finding, we also observed distinct topographical differences during the IDP epoch and subtle differences between PMdr and PMdc during the MOVE period (Fig. 7*B*). Specifically, during the IDP epoch PMdr showed a significantly greater mean discharge rate compared with PMdc for both conditions (Fig. 7*A*; $P < 0.01$). In line with the oscillatory activity results, the greatest mean discharge rate for PMdr was observed during the nonstandard condition, when the eyes and hand were decoupled (Figs. 6*B* and 8*A*; $P < 0.01$). Figure 8*B* shows that by late planning (early MOVE epoch), no significant topographical differences are evident during the standard condition ($P > 0.05$), and only minor differences are observed during the nonstandard condition. During this epoch we only observed clear topographical differences in the single-unit activity after movement onset (late MOVE epoch) and restricted to the standard condition (Fig. 7*B*; $P < 0.01$). Despite some minor differences from the LFP findings, the single-unit activity supports the hypothesis that functional differences exist between PMdr and PMdc and how they contribute to the performance of visuomotor transformations.

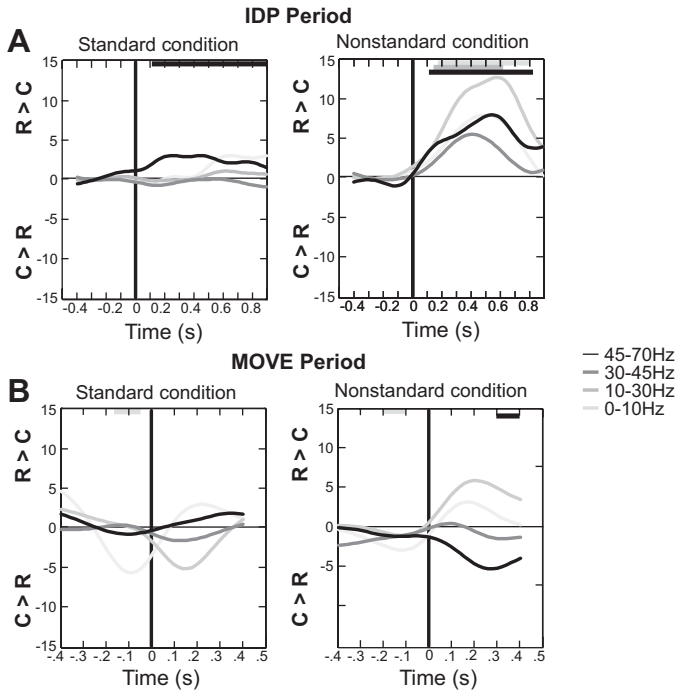

Fig. 8. Topographical difference in oscillatory activity during the IDP (*A*) and MOVE epochs (*B*). Positive *z*-score values reflect stronger oscillatory activity within PMdr, whereas negative *z*-score values represent stronger activity within PMdc. Vertical black bars represent onset of peripheral cue (*A*) and movement onset (*B*). R > C, activity in rostral PMd is stronger than in caudal PMd; C > R, activity in caudal PMd is stronger than in rostral PMd.

Gaze Effects

In an effort to determine whether the changes in oscillatory and single-unit activity between conditions arose solely from the shift in gaze angle attributable to the different viewing planes, a gaze-only condition was analyzed (see METHODS). Since the visual display in the nonstandard condition was presented on a vertical monitor and that in the standard condition was presented on a horizontal monitor, the animal's overall gaze angle (but not head position) changed between conditions. During the gaze-only condition, the animal fixated nine points on the horizontal and vertical screens. These fixation points corresponded to the location of the targets in the experimental conditions. The animal was instructed to fixate the points while maintaining its hands on levers to the side of the monitor. Any significant difference observed between conditions was considered to be related to gaze effects.

Within both PMdr and PMdc, no effects of gaze were observed for the frequency bands we tested (0–70 Hz; Fig. 9; $P > 0.05$). These data suggest that the changes we observed in oscillatory activity between standard and nonstandard condi-

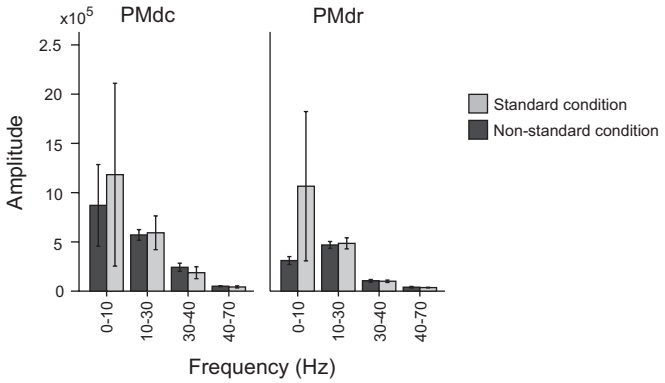

Fig. 9. Gaze control analysis. Values are mean amplitude and SD during standard and nonstandard conditions for PMdr (*A*) and PMdc (*B*). Bootstrapping methods revealed no significant difference in overall activity between conditions for each region ($P > 0.05$).

tions were not attributable solely to changes in overall gaze angle between the experimental conditions.

DISCUSSION

We report two principal findings following an examination of oscillatory activity in PMd during coupled vs. decoupled visually guided reaches. First, we observed task-related differences in PMd. Second, topographical differences were seen in the spectral profiles from PMdr and PMdc, during both planning and execution of standard and nonstandard reach. On the basis of our results, we suggest that the rostral portion of PMd plays a crucial role in breaking the tight linkage that exists for eye-hand coordination, whereas the caudal portion of the PMd plays a role in monitoring and updating the ongoing decoupled movement. We provide physiological data supporting previous anatomic work that suggest distinct roles for PMdr and PMdc in the control of visually guided reaching movements.

Task-Related Differences in PMd: Oscillatory Activity

In the present study, our nonstandard task required a decoupling of the eyes and the hand to different spatial locations, while the hand movements between conditions were biomechanically equivalent. Thus our nonstandard condition required a learned association. PMd is integral to the planning of conditional sensorimotor tasks, and lesions lead to impaired performance on these tasks (Chen and Wise 1995; Halsband and Passingham 1982, 1985; Petrides 1982, 1985, 1997; Wise et al. 1996). Consistent with our hypothesis, we observed that nonstandard reaches evoked region- and epoch-specific increases in oscillatory activity.

Similar to previous findings (Clavagnier et al. 2007; Gail et al. 2009; Prado et al. 2005), PMdr was more active during the early planning phase of decoupled vs. coupled reaching movements both at the single-cell level and within the 30- to 70-Hz gamma range. Oscillations within premotor regions are poorly understood. However, on the basis of general principles of cortical microcircuits, power increases in the gamma range may be attributed to increased or surplus local synchrony (Denker et al. 2011; Pesaran et al. 2002; von Stein and Sarnthein 2000). When combined with known anatomic connectivity, we suggest that this increase in gamma power within PMdr could be related to the additional cognitive processes, such as spatial working memory and divided attention, putatively required for nonstandard movements. These data also support behavioral evidence suggesting that an increase in neural processing is necessary during nonstandard visuomotor transformations (Gorbet and Sergio 2009).

The ability to perform decoupled reaching movements likely requires communication between prefrontal and premotor regions (Abe and Hanakawa 2009; Hoshi 2006; Hoshi and Tanji 2000). The dorsolateral prefrontal cortex (DLPFC) and PMdr are highly interconnected (Lu et al. 1994; Tachibana et al. 2004) and become functionally coupled either when a motor plan requires the integration of a diverse set of instructions (Abe and Hanakawa 2009; Hoshi 2006; Hoshi and Tanji 2000) or during cognitive manipulations (Abe and Hanakawa 2009). The increase in information received by PMdr to plan decoupled reaches would require enhanced local processing and integration and might thus be reflected in the increased gamma oscillatory activity that occurs within PMdr during the nonstandard condition. Similarly, if PMdc cells are important particularly when planning a "decoupled" movement, one might expect the observed enhancement in gamma synchrony during the early planning phase of decoupled movements in PMdc, which is absent in our results during the early planning period. Gamma-band oscillations are, however, observed within PMdc during the movement epoch of nonstandard compared with standard reaches (Fig. 5*D*). Consistent with the commonly suggested function of gamma oscillations (Denker et al. 2011; Pesaran et al. 2002; von Stein and Sarnthein 2000), the enhanced local synchrony that is occurring during a decoupled reach may reflect the online monitoring of the ballistic motor plan. Executing a nonstandard reach requires the actions of the eyes and the hand to remain decoupled and thus requires additional online reach monitoring and movement guidance using proprioceptive or somesthetic feedback. Area PEc located within the anterior portion of the superior parietal lobule houses somatosensory cells (Breveglieri et al. 2006; Kalaska 1996; Weinrich et al. 1984) and has a strong anatomic connection with area PMdc (Johnson et al. 1996). This is consistent with our oscillatory results demonstrating stronger oscillatory power within the 45- to 70-Hz gamma range in PMdc compared with PMdr during decoupled reaches (Fig. 8*B*). Additionally, only modest increases in gamma oscillations were observed during standard reaching movements, where the reliance on proprioceptive inputs is not as crucial relative to decoupled eye-hand situations. Decoupled reaches also require a signal that inhibits the natural tendency to link the movements of the eyes and the hand. Recently, Gail et al. (2009) suggested that the enhanced spiking activity observed in PMd during a nonstandard reaching movement reflects such an inhibiting signal to overrule the "default" visuomotor network for standard reaches (Everling et al. 1999; Gail et al. 2009; Schlag-Rey et al. 1997). This is in line with our spike data, which also demonstrate an increase in the discharge rate of single cells during the planning phase of nonstandard reaching movements. For PMdr to provide an inhibitory output signal, it must first be able to receive information about the spatial disparity between gaze and limb position. The enhanced oscillatory activity observed within PMdr during nonstandard reach planning may serve this purpose, which may then drive the increase in output signals (single units) that would be needed to inhibit the "default" visuomotor network, as suggested by others (Gail et al. 2009; Gorbet et al. 2004). Such an arrangement would make PMdr a crucial node in the sensorimotor transformation of nonstandard limb movements, although this interpretation raises further questions. In contrast, PMdc demonstrates a decrease in oscillatory activity during nonstandard relative to standard reach planning. This reduction in power may represent inhibitory inputs to PMdc, which would be important for allowing the eyes and hand to decouple. Recently, we have found that the mean discharge in single cells recorded from superior parietal areas during the same experiment presented here is significantly reduced during nonstandard task planning (Hawkins et al. 2013). The decoupling of goal/gaze spatial location and sensed limb location may underlie the reduction in activity in these bimodal cells. The subsequent transmission of these signals to premotor planning areas, observable in the input-driven LFP signal, may thus represent the crucial transformation of information that would

be needed to decouple the actions of the limb and gaze to successfully perform the task used in these studies.

If the role of PMd is to instruct or inhibit other regions during nonstandard conditions, and across-region or more "global" synchronization is associated with lower frequency oscillations, then one might expect an increase in beta and lower frequencies for the nonstandard task. Subgamma frequencies including beta are observed when a region is integrating independent distant signals or for "top down" processing as opposed to engaging in local processing (Donner and Siegel 2011; Siegel et al. 2012). Consistent with this, our results demonstrate that within PMdr there is an increase in low-frequency power during the early planning period of a nonstandard compared with a standard movement (Fig. 5*B*). On the basis of the aforementioned idea, the increase in low-frequency power seen in the early planning period of a nonstandard reach may reflect the integration of the cognitive rule into the motor action, allowing for a new relative position code of the eyes and hand.

Contrary to these observations, PMdc showed a reduction in low-frequency power during the planning and movement periods in the nonstandard condition (notice both epochs, Fig. 5, *A* and *B*). Under natural reaching situations, the brain must integrate hand and eye signals to arrive at the proper behavior, as in the standard version of the task. Perhaps within PMdc, performance during the nonstandard condition requires that these signals continue to be segregated, not integrated, just as the planes of movement of the hand and eyes are separated in space. Thus, although PMdr normally functions to integrate the signals from various regions of the brain for successful eye-hand decoupling, the suppression of beta or lower frequencies would be expected during nonstandard reaching within PMdc if this is an area of importance for eye-hand coupling. Cautious interpretation is warranted, however, since the oscillatory functions within PMd are largely unknown, and the present results suggest a complex repertoire of oscillations that reveal temporal and spectral differences even within PMd.

Functional and Anatomic Separation Within PMd

Most PMd single-unit studies have not separated PMd into its rostral-caudal subdivisions. A reexamination of the literature has revealed that the majority of cells that respond to conditional visuomotor associations appear to be located within PMdr, whereas cells within PMdc demonstrate mostly movement-related activity (Grafton et al. 1998; Picard and Strick 2001). The authors of these reviews suggest the term "pre-PMd" for PMdr, reflecting the cognitive conditional visuomotor associations that have been commonly observed there. The functional separation in the activity of PMd cell assemblies in the current study support this proposed distinction: PMdr was more active during decoupled reaching movements, when the movement relied on a transformational rule to be incorporated into the reaching movement. By the late planning/early movement phase of both standard and nonstandard movements, PMdc had stronger oscillatory and single-unit activity. During this period concerned with movement execution rather than planning, the salient features would be the biomechanical details of the movement, which did not vary with task in the present study (Boussaoud 2001; Picard and Strick 2001; Scott and Kalaska 1997; Scott et al. 1997; Toni et al. 2001). Left open is the question of how information within PMdr affects the final movement programming in PMdc, supplementary motor area (SMA), M1, or spinal cord structures, given the evidence that there are few if any direct connections between PMdr and these other areas (Barbas and Pandya 1987; Kurata 1991; Luppino and Rizzolatti 2000; Tachibana et al. 2004). It has been suggested that PMdr, a rostral motor region, plays a large role in relaying prefrontal signals to pre-SMA and rostral cingulate motor area (CMAr) to eventually reach the more caudal motor regions such as SMA, PMdc, and finally M1 (Lu et al. 1994; Morecraft et al. 2004; Takada et al. 2004). These connections are important because they may provide a pathway for information flow from DLPFC and PMdr, and thus allow signals important for decoupled reaching to reach the final motor plan. Another avenue for PMdr activity to influence the motor plan may be via the corticostriatal connections between PMdr and the basal ganglia (BG) (Tachibana et al. 2004). Considering that PMdr is thought to play a role in inhibiting the natural tendency to couple the eyes and hand during decoupled reaching movements (Gail et al. 2009; Gorbet et al. 2004), its connection with BG structures may help mediate the inhibitory signal that would be necessary to accomplish this type of reaching movement. Recently, SMA has been shown to play a key role in proactive control, the ability to stop a movement based on endogenous signals (Chen et al. 2010; Jaffard et al. 2008). Proactive control is key to our ability to inhibit our natural tendency to couple the eyes and the hand. Thus this region may also play a key role in our ability to decouple the eyes and hand. Finally, based on the strong reciprocal connections that the premotor and parietal cortices share (Geyer et al. 2000; Lu et al. 1994; Luppino and Rizzolatti 2000; Matelli et al. 1998; Pandya and Yeterian 1984; Picard and Strick 2001), information from PMdr may provide the parietal lobe with signals necessary to incorporate a rule into the ongoing movement.

In conclusion, the task-related oscillatory activity in PMd observed in the present study supports necessary but separate roles for rostral and caudal subregions in the control of nonstandard reaching, a behavior performed in everyday life. PMdr activity appears to be more involved in integrating the rule-based aspects of a visually guided reach, whereas PMdc is more involved in the online updating of the decoupled eye and hand movements. We propose that PMd, particularly the rostral portion, plays a crucial role in breaking the tight linkage that exists for eye-hand coupling. We also provide physiological data that suggest distinct roles for PMdr and PMdc in the control of visually guided reaching movements. On a practical level, these results indicate that caution should be taken when comparing data obtained from studies using direct object manipulation with those from studies using nonstandard, decoupled target/object interaction.

ACKNOWLEDGMENTS

We thank Taiwo McGregor, Tyrone Lew, Dr. Xiaogang Yan, Dr. Bogdan Neagu, and Dr. Hongying Wang for exceptional technical and surgical assistance, as well as Natasha Down, Veronica Scavo, and Julie Panakos for invaluable animal care expertise.

GRANTS

This work was supported by Canadian Institutes of Health Research Grant MOP-74634 (to L. E. Sergio), the Canadian Foundation for Innovation and the

Ontario Innovation Trust (to L. E. Sergio), and the Ontario Ministry of Training, Colleges, and Universities (Ontario Graduate Scholarship in Science and Technology to P. F. Sayegh).

DISCLOSURES

No conflicts of interest, financial or otherwise, are declared by the authors.

AUTHOR CONTRIBUTIONS

P.F.S., K.M.H., and L.E.S. performed experiments; P.F.S., K.L.H., and L.E.S. analyzed data; P.F.S., K.L.H., and L.E.S. interpreted results of experiments; P.F.S. prepared figures; P.F.S. drafted manuscript; P.F.S., K.M.H., K.L.H., and L.E.S. edited and revised manuscript; P.F.S., K.M.H., K.L.H., and L.E.S. approved final version of manuscript; L.E.S. conception and design of research.

REFERENCES

Abe M, Hanakawa T. Functional coupling underlying motor and cognitive functions of the dorsal premotor cortex. *Behav Brain Res* 198: 13–23, 2009.

Alexander GE, Crutcher MD. Preparation for movement: neural representations of intended direction in three motor areas of the monkey. *J Neurophysiol* 64: 133–150, 1990.

Baker SN, Kilner JM, Pinches EM, Lemon RN. The role of synchrony and oscillations in the motor output. *Exp Brain Res* 128: 109–117, 1999.

Barbas H, Pandya DN. Architecture and frontal cortical connections of the premotor cortex (area 6) in the rhesus monkey. *J Comp Neurol* 256: 211–228, 1987.

Battaglia-Mayer A, Ferraina S, Genovesio A, Marconi B, Squatrito S, Molinari M, Lacquaniti F, Caminiti R. Eye-hand coordination during reaching. II. An analysis of the relationships between visuomanual signals in parietal cortex and parieto-frontal association projections. *Cereb Cortex* 11: 528–544, 2001.

Bo J, Contreras-Vidal JL, Kagerer FA, Clark JE. Effects of increased complexity of visuo-motor transformations on children's arm movements. *Hum Mov Sci* 25: 553–567, 2006.

Boussaoud D. Attention versus intention in the primate premotor cortex. *Neuroimage* 14: S40–S45, 2001.

Boussaoud D, Jouffrais C, Bremmer F. Eye position effects on the neuronal activity of dorsal premotor cortex in the macaque monkey. *J Neurophysiol* 80: 1132–1150, 1998.

Boussaoud D, Wise SP. Primate frontal cortex: effects of stimulus and movement. *Exp Brain Res* 95: 28–40, 1993a.

Boussaoud D, Wise SP. Primate frontal cortex: neuronal activity following attentional versus intentional cues. *Exp Brain Res* 95: 15–27, 1993b.

Breveglieri R, Galletti C, Gamberini M, Passarelli L, Fattori P. Somatosensory cells in area PEc of macaque posterior parietal cortex. *J Neurosci* 26: 3679–3684, 2006.

Brovelli A, Lachaux JP, Kahane P, Boussaoud D. High gamma frequency oscillatory activity dissociates attention from intention in the human premotor cortex. *Neuroimage* 28: 154–164, 2005.

Caminiti R, Genovesio A, Marconi B, Battaglia-Mayer A, Onorati P, Ferraina S, Mitsuda T, Giannetti S, Squatrito S, Maioli M, Molinari M. Early coding of reaching: frontal and parietal association connections of parieto-occipital cortex. *Eur J Neurosci* 11: 3339–3345, 1999.

Caminiti R, Johnson PB, Burnod Y, Galli C, Ferraina S. Shift of preferred directions of premotor cortical cells with arm movements performed across the workspace. *Exp Brain Res* 83: 228–232, 1990.

Chen LL, Wise SP. Neuronal activity in the supplementary eye field during acquisition of conditional oculomotor associations. *J Neurophysiol* 73: 1101–1121, 1995.

Chen X, Scangos KW, Stuphorn V. Supplementary motor area exerts proactive and reactive control of arm movements. *J Neurosci* 30: 14657–14675, 2010.

Cisek P, Crammond DJ, Kalaska JF. Neural activity in primary motor and dorsal premotor cortex in reaching tasks with the contralateral versus ipsilateral arm. *J Neurophysiol* 89: 922–942, 2003.

Cisek P, Kalaska JF. Neural correlates of reaching decisions in dorsal premotor cortex: specification of multiple direction choices and final selection of action. *Neuron* 45: 801–814, 2005.

Cisek P, Kalaska JF. Modest gaze-related discharge modulation in monkey dorsal premotor cortex during a reaching task performed with free fixation. *J Neurophysiol* 88: 1064–1072, 2002.

Clavagnier S, Prado J, Kennedy H, Perenin MT. How humans reach: distinct cortical systems for central and peripheral vision. *Neuroscientist* 13: 22–27, 2007.

Cooper NR, Croft RJ, Dominey SJ, Burgess AP, Gruzelier JH. Paradox lost? Exploring the role of alpha oscillations during externally vs internally directed attention and the implications for idling and inhibition hypotheses. *Int J Psychophysiol* 47: 65–74, 2003.

Denker M, Roux S, Linden H, Diesmann M, Riehle A, Grun S. The local field potential reflects surplus spike synchrony. *Cereb Cortex* 21: 2681–2695, 2011.

Donner TH, Siegel M. A framework for local cortical oscillation patterns. *Trends Cogn Sci* 15: 191–199, 2011.

Donoghue JP, Sanes JN, Hatsopoulos NG, Gaal G. Neural discharge and local field potential oscillations in primate motor cortex during voluntary movements. *J Neurophysiol* 79: 159–173, 1998.

Epelboim J, Steinman RM, Kowler E, Pizlo Z, Erkelens CJ, Collewijn H. Gaze-shift dynamics in two kinds of sequential looking tasks. *Vision Res* 37: 2597–2607, 1997.

Everling S, Dorris MC, Klein RM, Munoz DP. Role of primate superior colliculus in preparation and execution of anti-saccades and pro-saccades. *J Neurosci* 19: 2740–2754, 1999.

Fries P, Reynolds JH, Rorie AE, Desimone R. Modulation of oscillatory neuronal synchronization by selective visual attention. *Science* 291: 1560–1563, 2001.

Fujii N, Mushiake H, Tanji J. Rostrocaudal distinction of the dorsal premotor area based on oculomotor involvement. *J Neurophysiol* 83: 1764–1769, 2000.

Gail A, Klaes C, Westendorff S. Implementation of spatial transformation rules for goal-directed reaching via gain modulation in monkey parietal and premotor cortex. *J Neurosci* 29: 9490–9499, 2009.

Gauthier GM, Mussa Ivaldi F. Oculo-manual tracking of visual targets in monkey: role of the arm afferent information in the control of arm and eye movements. *Exp Brain Res* 73: 138–154, 1988.

Georgopoulos AP, Kalaska JF, Caminiti R, Massey JT. On the relations between the direction of two-dimensional arm movements and cell discharge in primate motor cortex. *J Neurosci* 2: 1527–1537, 1982.

Geyer S, Matelli M, Luppino G, Zilles K. Functional neuroanatomy of the primate isocortical motor system. *Anat Embryol (Berl)* 202: 443–474, 2000.

Ghilardi MF, Alberoni M, Marelli S, Rossi M, Franceschi M, Ghez C, Fazio F. Impaired movement control in Alzheimer's disease. *Neurosci Lett* 260: 45–48, 1999.

Gielen CC, van den Heuvel PJ, van Gisbergen JA. Coordination of fast eye and arm movements in a tracking task. *Exp Brain Res* 56: 154–161, 1984.

Goense JB, Logothetis NK. Neurophysiology of the BOLD fMRI signal in awake monkeys. *Curr Biol* 18: 631–640, 2008.

Goodbody SJ, Wolpert DM. The effect of visuomotor displacements on arm movement paths. *Exp Brain Res* 127: 213–223, 1999.

Gorbet DJ, Sergio LE. The behavioural consequences of dissociating the spatial directions of eye and arm movements. *Brain Res* 1284: 77–88, 2009.

Gorbet DJ, Staines WR, Sergio LE. Brain mechanisms for preparing increasingly complex sensory to motor transformations. *Neuroimage* 23: 1100–1111, 2004.

Gordon J, Ghilardi MF, Cooper SE, Ghez C. Accuracy of planar reaching movements. II. Systematic extent errors resulting from inertial anisotropy. *Exp Brain Res* 99: 112–130, 1994.

Grafton ST, Fagg AH, Arbib MA. Dorsal premotor cortex and conditional movement selection: a PET functional mapping study. *J Neurophysiol* 79: 1092–1097, 1998.

Halsband U, Passingham R. The role of premotor and parietal cortex in the direction of action. *Brain Res* 240: 368–372, 1982.

Halsband U, Passingham RE. Premotor cortex and the conditions for movement in monkeys (*Macaca fascicularis*). *Behav Brain Res* 18: 269–277, 1985.

Hawkins KM, Sayegh P, Yan X, Crawford JD, Sergio LE. Neural activity in superior parietal cortex during rule-based visual-motor transformations. *J Cogn Neurosci* 25: 436–454, 2013.

Henriques DY, Klier EM, Smith MA, Lowy D, Crawford JD. Gaze-centered remapping of remembered visual space in an open-loop pointing task. *J Neurosci* 18: 1583–1594, 1998.

Hoshi E. Functional specialization within the dorsolateral prefrontal cortex: A review of anatomical and physiological studies of non-human primates. *Neurosci Res* 54: 73, 2006.

Hoshi E, Tanji J. Integration of target and body-part information in the premotor cortex when planning action. *Nature* 408: 466–470, 2000.

Jackson SR, Newport R, Mort D, Husain M. Where the eye looks, the hand follows; limb-dependent magnetic misreaching in optic ataxia. *Curr Biol* 15: 42–46, 2005.

Jaffard M, Longcamp M, Velay JL, Anton JL, Roth M, Nazarian B, Boulinguez P. Proactive inhibitory control of movement assessed by event-related fMRI. *Neuroimage* 42: 1196–1206, 2008.

Jarvis MR, Mitra PP. Sampling properties of the spectrum and coherency of sequences of action potentials. *Neural Comput* 13: 717–749, 2001.

Jensen O, Kaiser J, Lachaux JP. Human gamma-frequency oscillations associated with attention and memory. *Trends Neurosci* 30: 317–324, 2007.

Johnson PB, Ferraina S, Bianchi L, Caminiti R. Cortical networks for visual reaching: physiological and anatomical organization of frontal and parietal lobe arm regions. *Cereb Cortex* 6: 102–119, 1996.

Kalaska JF. Parietal cortex area 5 and visuomotor behavior. *Can J Physiol Pharmacol* 74: 483–498, 1996.

Kalaska JF, Cohen DA, Hyde ML, Prud'homme M. A comparison of movement direction-related versus load direction-related activity in primate motor cortex, using a two-dimensional reaching task. *J Neurosci* 9: 2080–2102, 1989.

Kalaska JF, Sergio LE, Cisek P. Cortical control of whole-arm motor tasks. *Novartis Found Symp* 218: 176–190, 1998.

Karnath HO, Perenin MT. Cortical control of visually guided reaching: evidence from patients with optic ataxia. *Cereb Cortex* 15: 1561–1569, 2005.

Kurata K. Corticocortical inputs to the dorsal and ventral aspects of the premotor cortex of macaque monkeys. *Neurosci Res* 12: 263–280, 1991.

Lu MT, Preston JB, Strick PL. Interconnections between the prefrontal cortex and the premotor areas in the frontal lobe. *J Comp Neurol* 341: 375–392, 1994.

Luppino G, Matelli M, Rizzolatti G. Cortico-cortical connections of two electrophysiologically identified arm representations in the mesial agranular frontal cortex. *Exp Brain Res* 82: 214–218, 1990.

Luppino G, Rizzolatti G. The organization of the frontal motor cortex. *News Physiol Sci* 15: 219–224, 2000.

Matelli M, Govoni P, Galletti C, Kutz DF, Luppino G. Superior area 6 afferents from the superior parietal lobule in the macaque monkey. *J Comp Neurol* 402: 327–352, 1998.

Messier J, Kalaska JF. Differential effect of task conditions on errors of direction and extent of reaching movements. *Exp Brain Res* 115: 469–478, 1997.

Mitzdorf U. Current source-density method and application in cat cerebral cortex: investigation of evoked potentials and EEG phenomena. *Physiol Rev* 65: 37–100, 1985.

Morasso P. Spatial control of arm movements. *Exp Brain Res* 42: 223–227, 1981.

Morecraft RJ, Cipolloni PB, Stilwell-Morecraft KS, Gedney MT, Pandya DN. Cytoarchitecture and cortical connections of the posterior cingulate and adjacent somatosensory fields in the rhesus monkey. *J Comp Neurol* 469: 37–69, 2004.

Murray EA, Bussey TJ, Wise SP. Role of prefrontal cortex in a network for arbitrary visuomotor mapping. *Exp Brain Res* 133: 114–129, 2000.

Neggers SF, Bekkering H. Ocular gaze is anchored to the target of an ongoing pointing movement. *J Neurophysiol* 83: 639–651, 2000.

Nir Y, Fisch L, Mukamel R, Gelbard-Sagiv H, Arieli A, Fried I, Malach R. Coupling between neuronal firing rate, gamma LFP, and BOLD fMRI is related to interneuronal correlations. *Curr Biol* 17: 1275–1285, 2007.

O'Leary JG, Hatsopoulos NG. Early visuomotor representations revealed from evoked local field potentials in motor and premotor cortical areas. *J Neurophysiol* 96: 1492–1506, 2006.

Pandya DN, Yeterian EH. Proposed neural circuitry for spatial memory in the primate brain. *Neuropsychologia* 22: 109–122, 1984.

Paxinos G, Huang XF, Toga AW. *The Rhesus Monkey Brain in Stereotaxic Coordinates*. San Diego, CA: Academic, 2000.

Pesaran B, Pezaris JS, Sahani M, Mitra PP, Andersen RA. Temporal structure in neuronal activity during working memory in macaque parietal cortex. *Nat Neurosci* 5: 805–811, 2002.

Petrides M. Visuo-motor conditional associative learning after frontal and temporal lesions in the human brain. *Neuropsychologia* 35: 989–997, 1997.

Petrides M. Deficits on conditional associative-learning tasks after frontal- and temporal-lobe lesions in man. *Neuropsychologia* 23: 601–614, 1985.

Petrides M. Motor conditional associative-learning after selective prefrontal lesions in the monkey. *Behav Brain Res* 5: 407–413, 1982.

Piaget J. *The Construction of Reality in the Child*. New York: Basic Books, 1965.

Picard N, Strick PL. Imaging the premotor areas. *Curr Opin Neurobiol* 11: 663–672, 2001.

Prablanc C, Echallier JF, Komilis E, Jeannerod M. Optimal response of eye and hand motor systems in pointing at a visual target. I. Spatio-temporal characteristics of eye and hand movements and their relationships when varying the amount of visual information. *Biol Cybern* 35: 113–124, 1979.

Prado J, Clavagnier S, Otzenberger H, Scheiber C, Kennedy H, Perenin MT. Two cortical systems for reaching in central and peripheral vision. *Neuron* 48: 849–858, 2005.

Raos V, Umilta MA, Gallese V, Fogassi L. Functional properties of grasping-related neurons in the dorsal premotor area F2 of the macaque monkey. *J Neurophysiol* 92: 1990–2002, 2004.

Ray S, Maunsell JH. Different origins of gamma rhythm and high-gamma activity in macaque visual cortex. *PLoS Biol* 9: e1000610, 2011.

Sanes JN, Donoghue JP. Oscillations in local field potentials of the primate motor cortex during voluntary movement. *Proc Natl Acad Sci USA* 90: 4470–4474, 1993.

Scherberger H, Jarvis MR, Andersen RA. Cortical local field potential encodes movement intentions in the posterior parietal cortex. *Neuron* 46: 347–354, 2005.

Schlag-Rey M, Amador N, Sanchez H, Schlag J. Antisaccade performance predicted by neuronal activity in the supplementary eye field. *Nature* 390: 398–401, 1997.

Scott SH, Kalaska JF. Reaching movements with similar hand paths but different arm orientations. I. Activity of individual cells in motor cortex. *J Neurophysiol* 77: 826–852, 1997.

Scott SH, Sergio LE, Kalaska JF. Reaching movements with similar hand paths but different arm orientations. II. Activity of individual cells in dorsal premotor cortex and parietal area 5. *J Neurophysiol* 78: 2413–2426, 1997.

Sergio LE, Gorbet DJ, Tippett WJ, Yan X, Neagu B. Cortical mechanisms of vision for complex action. In: *Cortical Mechanisms of Vision*, edited by Jenkins M and Harris L. Cambridge, UK: Cambridge University Press, 2009.

Sergio LE, Kalaska JF. Systematic changes in motor cortex cell activity with arm posture during directional isometric force generation. *J Neurophysiol* 89: 212–228, 2003.

Sergio LE, Scott SH. Hand and joint paths during reaching movements with and without vision. *Exp Brain Res* 122: 157–164, 1998.

Siegel M, Donner TH, Engel AK. Spectral fingerprints of large-scale neuronal interactions. *Nat Rev Neurosci* 13: 121–134, 2012.

Snedecor GW, Cochrane WG. *Statistical Methods*. Ames, IA: Blackwell, 1989.

Tachibana Y, Nambu A, Hatanaka N, Miyachi S, Takada M. Input-output organization of the rostral part of the dorsal premotor cortex, with special reference to its corticostriatal projection. *Neurosci Res* 48: 45–57, 2004.

Takada M, Nambu A, Hatanaka N, Tachibana Y, Miyachi S, Taira M, Inase M. Organization of prefrontal outflow toward frontal motor-related areas in macaque monkeys. *Eur J Neurosci* 19: 3328–3342, 2004.

Terao Y, Andersson NE, Flanagan JR, Johansson RS. Engagement of gaze in capturing targets for future sequential manual actions. *J Neurophysiol* 88: 1716–1725, 2002.

Tippett WJ, Krajewski A, Sergio LE. Visuomotor integration is compromised in Alzheimer's disease patients reaching for remembered targets. *Eur Neurol* 58: 1–11, 2007.

Tippett WJ, Sergio LE. Visuomotor integration is impaired in early stage Alzheimer's disease. *Brain Res* 1102: 92–102, 2006.

Toni I, Rushworth MF, Passingham RE. Neural correlates of visuomotor associations. Spatial rules compared with arbitrary rules. *Exp Brain Res* 141: 359–369, 2001.

Vercher JL, Magenes G, Prablanc C, Gauthier GM. Eye-head-hand coordination in pointing at visual targets: spatial and temporal analysis. *Exp Brain Res* 99: 507–523, 1994.

von Stein A, Sarnthein J. Different frequencies for different scales of cortical integration: from local gamma to long range alpha/theta synchronization. *Int J Psychophysiol* 38: 301–313, 2000.

Weinrich M, Wise SP, Mauritz KH. A neurophysiological study of the premotor cortex in the rhesus monkey. *Brain* 107: 385–414, 1984.

Wise SP, di Pellegrino G, Boussaoud D. The premotor cortex and nonstandard sensorimotor mapping. *Can J Physiol Pharmacol* 74: 469–482, 1996.

Zanos S, Zanos TP, Marmarelis VZ, Ojemann GA, Fetz EE. Relationships between spike-free local field potentials and spike timing in human temporal cortex. *J Neurophysiol* 107: 1808–1821, 2012.

Zanos TP, Mineault PJ, Pack CC. Removal of spurious correlations between spikes and local field potentials. *J Neurophysiol* 105: 474–486, 2011.